

Gapless excitations in non-Abelian Kitaev spin liquids with line defects

Lucas R. D. Freitas¹ and Rodrigo G. Pereira^{1,2}

¹*Departamento de Física Teórica e Experimental,*

Universidade Federal do Rio Grande do Norte, Natal, RN, 59078-970, Brazil

²*International Institute of Physics, Universidade Federal do Rio Grande do Norte, Natal, RN, 59078-970, Brazil*

We show that line defects in a non-Abelian Kitaev spin liquid harbor gapless one-dimensional Majorana modes if the interaction across the defect falls below a critical value. Treating the weak interaction at the line defect within a mean-field approximation, we determine the critical interaction strength as a function of the external magnetic field. In the gapless regime, we use the low-energy effective field theory to calculate the spin-lattice relaxation rate for a nuclear spin near the defect and find a cubic temperature dependence that agrees with experiments in the Kitaev material α -RuCl₃.

Introduction.—The Kitaev honeycomb model [1] provides a prominent example of a quantum spin liquid [2–4] in which spins fractionalize into emergent Majorana fermions. In the presence of a magnetic field, the phase diagram of the model includes a non-Abelian phase characterized by gapped bulk excitations and chiral edge states [1]. The observation that an extended Kitaev model can be realized in strongly spin-orbit-coupled Mott insulators [5–7] led to the discovery of candidate materials, including the iridates [8–10] and α -RuCl₃ [11–14]. In the latter, the suppression of long-range zigzag order above a critical value of an in-plane magnetic field [15] has been interpreted in terms of a field-induced gapped spin liquid, with supporting evidence from thermal Hall [16, 17] and specific heat measurements [18].

The inevitable presence of defects in real materials both complicates and enriches the physics of Kitaev spin liquids [19–25]. Quite generally, disorder tends to modify the low-energy density of states in a way that may overshadow universal properties predicted for the clean system. For instance, single vacancies and magnetic impurities can bind vortices of the \mathbb{Z}_2 gauge field and Majorana zero modes [19, 20]. A finite density of vacancies and bond randomness can account for the divergent low-energy density of states in H₃LiIr₂O₆ [10, 21].

In this work, we investigate line defects, such as dislocations and grain boundaries [26], in the non-Abelian Kitaev spin liquid. Such one-dimensional (1D) defects can be engineered in monolayers of 2D materials [27] and their orientation depends on strain [28]. In bulk crystals, partial dislocations naturally appear bordering stacking faults [26], which are ubiquitous in α -RuCl₃ due to the weak van der Waals bonding between layers [29–31]. Dislocations in the gapped Abelian phase of the anisotropic Kitaev model were studied in Refs. [32, 33].

We model the 1D defect as a line of weaker exchange bonds as shown in Fig. 1(a). For defect interaction $\tilde{J} = 0$, the system reduces to two decoupled Kitaev spin liquids with zigzag edges. In the non-Abelian phase, the decoupled edges harbor gapless chiral Majorana modes. Aasen *et al.* [34] noted that there is a critical value of the interaction below which these 1D modes remain gapless.

The reason is that the leading interaction between emergent Majorana fermions across the interface is irrelevant in the renormalization group sense. In addition to the effective field theory, the problem of seaming two Kitaev spin liquids was analyzed in Ref. [34] by analogy with 1D lattice models that exhibit a transition in the same universality class [35]. Here we start from the Kitaev model and calculate the spectrum using a self-consistent mean-field approximation for the interaction along the defect. Our approach reveals that the critical coupling stems from a competition between this interaction and the Zeeman coupling for the dangling-bond spins.

Below the critical coupling, the gapless Majorana modes along the line defect can dominate the low-energy behavior of local response functions. To illustrate this point, we calculate the spin-lattice relaxation rate $1/T_1$ within the effective field theory. We find $1/T_1 \propto T^3$ at low temperatures, in clear contrast with the exponential dependence expected for a gapped spin liquid. Remarkably, the cubic temperature dependence matches the result of the nuclear magnetic resonance (NMR) experiment in Ref. [36]. We then propose that the contribution from gapless 1D modes in samples with a low but finite

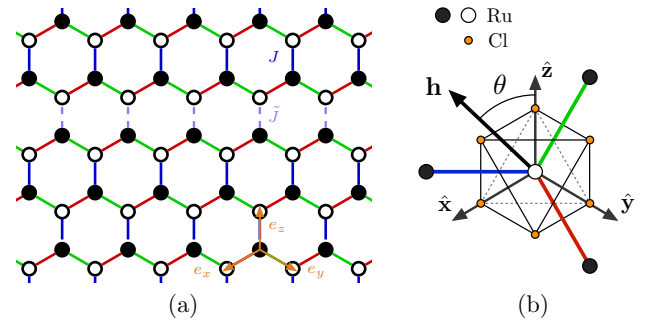


FIG. 1. Kitaev honeycomb model with a line defect. Black and white circles represent the sublattices. Nearest-neighbor x -, y - and z -bonds are colored in red, green and blue, respectively. (a) The coupling \tilde{J} along the defect is represented by dashed lines. The vectors $\mathbf{e}_{x,y,z}$ indicate the bond directions in the plane. (b) In α -RuCl₃, the Cartesian axes with unit vectors $\hat{\mathbf{x}}$, $\hat{\mathbf{y}}$ and $\hat{\mathbf{z}}$ are defined by the vertices of the ligand octahedra. The magnetic field forms an angle θ with $\hat{\mathbf{z}}$.

density of line defects might explain the discrepancy with other NMR experiments that observed a spin gap inside the putative Kitaev spin liquid phase [37–39].

Microscopic model.—Our starting point is the spin-1/2 Kitaev honeycomb model in a magnetic field [1]:

$$H = - \sum_{\langle j,k \rangle_\gamma} J_{jk} \sigma_j^\gamma \sigma_k^\gamma - \mathbf{h} \cdot \sum_j \boldsymbol{\sigma}_j. \quad (1)$$

Here $\boldsymbol{\sigma}_j$ is the vector of Pauli operators at site j . The Kitaev coupling on nearest-neighbor bonds of type $\gamma = x, y, z$ takes the value $J_{jk} = J$ in the bulk and $J_{jk} = \tilde{J} \ll J$ for the z bonds along the line defect, see Fig. 1(a). The nearest-neighbor vectors are $\mathbf{e}_x = (-\frac{1}{2}, -\frac{1}{2\sqrt{3}})$, $\mathbf{e}_y = (\frac{1}{2}, -\frac{1}{2\sqrt{3}})$ and $\mathbf{e}_z = (0, \frac{1}{\sqrt{3}})$, where we set the lattice parameter to unity. The components of the magnetic field $\mathbf{h} = h_x \hat{\mathbf{x}} + h_y \hat{\mathbf{y}} + h_z \hat{\mathbf{z}}$ are defined with respect to the axes fixed by the edge-sharing octahedra structure of α -RuCl₃ [40, 41]; see Fig. 1(b). Note that the z axis is perpendicular to the z bond. Importantly, even a small increase in the bond length across the defect can significantly suppress the Kitaev coupling [42]. Since the weaker coupling is the mechanism behind the persistence of gapless 1D modes, we consider an infinite line defect without specifying its detailed properties, *e.g.*, the Burgers vector of dislocations [32]. For simplicity, we neglect interactions beyond the pure Kitaev model [7, 43], which can renormalize the critical coupling discussed in the following, but do not change qualitative features of the transition or the temperature dependence of T_1^{-1} .

For $\mathbf{h} = 0$, the Kitaev model is solved by the representation $\sigma_j^\gamma = ib_j^\gamma c_j$, where b_j^γ and c_j are Majorana fermions [1]. To restrict to the physical spin-1/2 Hilbert space, one imposes the local constraint $b_j^x b_j^y b_j^z c_j = 1$ for all sites. There is one conserved quantity for each hexagonal plaquette p , given by $W_p = \prod_{\langle j,k \rangle \in \partial p} u_{jk}$, where $u_{jk} = ib_j^\gamma b_k^\gamma$ acts as a \mathbb{Z}_2 gauge field on the $\langle j,k \rangle_\gamma$ bond with site j in sublattice A (black circles in Fig. 1) and site k in sublattice B (white circles).

To make progress analytically, we follow Ref. [1] and replace the Zeeman coupling in the bulk by a three-spin interaction generated by perturbation theory in the magnetic field. This approach is justified by a projection onto the low-energy sector where $W_p = 1 \forall p$, which contains the exact ground state for $\mathbf{h} = 0$. In this sector, we can set $u_{jk} = 1$, freezing out all b^γ fermions in the bulk. Moreover, the three-spin interaction effectively gaps out the spectrum of c fermions with a topologically nontrivial mass, which is the main effect of time-reversal-symmetry breaking that we wish to capture with our model to describe the non-Abelian spin liquid phase. On the other hand, for $\tilde{J} = 0$, the b^z fermions associated with the broken z bonds, see Fig. 1(a), couple only to the c fermions through the Zeeman term proportional to h_z . In fact, for $\tilde{J} = 0$ there is no energy cost for changing W_p on plaquettes along the line defect. On defect sites we can

still integrate out the $b^{x,y}$ fermions, since these involve bonds with strong coupling J , but the b^z fermions remain dynamic at low energies. For this reason, we shall keep the projected Zeeman term on defect sites. As noted in Ref. [1], without this term the b^z fermions at an edge would decouple from the rest of the system and form a zero-energy flat band. The resulting Hamiltonian in the regime $|\mathbf{h}|, \tilde{J} \ll J$ is

$$H_{\text{eff}} = H_0 - \tilde{J} \sum_{j \in \ell_1} \sigma_j^z \sigma_{j+\mathbf{e}_z}^z - h_z \sum_{j \in \ell_1 \cup \ell_2} \sigma_j^z, \quad (2)$$

where $H_0 = -J \sum_{\langle j,k \rangle_\gamma} \sigma_j^\gamma \sigma_k^\gamma - \kappa \sum_{\langle j,k \rangle_\alpha, \langle k,l \rangle_\beta} \sigma_j^\alpha \sigma_k^\gamma \sigma_l^\beta$ contains the standard bulk interactions [1] and ℓ_1 and ℓ_2 refer to the lines of defect sites in A and B sublattices, respectively. The coupling constant of the three-spin interaction is related to the magnetic field by $\kappa \propto h_x h_y h_z / J^2$. Once we fix $u_{jk} = 1$ in the bulk, H_0 becomes a quadratic Hamiltonian for the c fermions with nearest- and next-nearest-neighbor couplings. In terms of Majorana fermions, we obtain

$$H_{\text{eff}} = H_0 - \tilde{J} \sum_{j \in \ell_1} b_j^z b_{j+\mathbf{e}_z}^z c_j c_{j+\mathbf{e}_z} - i h_z \sum_{j \in \ell_1 \cup \ell_2} b_j^z c_j. \quad (3)$$

Mean-field theory.—The model in Eq. (3) is not exactly solvable when both \tilde{J} and h_z are nonzero. While the Zeeman term is quadratic, the hybridization of b^z and c spoils the conservation of $ib_j^z b_k^z$ on defect bonds. Here we use a Majorana mean-field approximation for the quartic term. Similar approaches have been shown to capture phase transitions driven by integrability-breaking bulk interactions in the extended Kitaev model [44, 45]. We adopt the mean-field parameters $\chi_b = \langle ib_j^z b_{j+\mathbf{e}_z}^z \rangle$ and $\chi_c = \langle ic_j c_{j+\mathbf{e}_z} \rangle$ for $j \in \ell_1$. Performing a mean-field decoupling of the interaction $V = \tilde{J} \sum_{j \in \ell_1} (ib_j^z b_{j+\mathbf{e}_z}^z)(ic_j c_{j+\mathbf{e}_z})$, we obtain

$$V_{\text{MF}} = \tilde{J} \sum_{j \in \ell_1} (i\chi_c b_j^z b_{j+\mathbf{e}_z}^z + i\chi_b c_j c_{j+\mathbf{e}_z} - \chi_b \chi_c). \quad (4)$$

The replacement of V by V_{MF} in Eq. (3) yields the mean-field Hamiltonian H_{MF} .

We diagonalize the mean-field Hamiltonian numerically on a finite system with periodic boundary conditions. The geometry can be viewed as a torus with length L_x in the direction parallel to the line defect, along which the model has translational invariance, and containing L_y sites in the transverse direction. Representing a site by a pair of coordinates $j = (x, y)$, we define the Fourier transformed fermions

$$d_{q,y} = \frac{1}{\sqrt{2L_x}} \sum_{x=1}^{L_x} e^{-iqx} d_{x,y}, \quad y = 0, \dots, L_y + 1, \quad (5)$$

where $d_{x,y} = c_{x,y}$ for $y = 1, \dots, L_y$, $d_{x,0} = b_{x,1}^z$ and $d_{x,L_y+1} = b_{x,L_y}^z$. In this notation, $y = 1$ and $y = L_y$

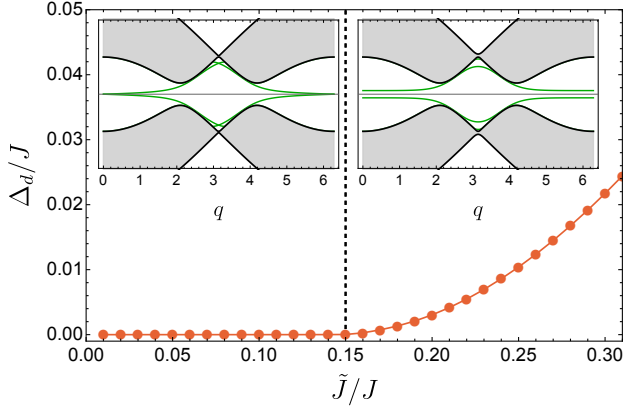


FIG. 2. Energy gap for the Majorana modes bound to the line defect as a function of the modified coupling \tilde{J} . Here we fix the magnetic field along the [111] direction with $|\mathbf{h}| = 0.8J$. The dashed line indicates the critical coupling \tilde{J}_c . The inset shows the spectrum below and above \tilde{J}_c . The green lines refer to defect modes and the continuum to gapped bulk modes.

correspond to lines ℓ_1 and ℓ_2 , respectively. The mean-field Hamiltonian is quadratic in the complex fermions $d_{q,y}$ and can be cast in the form

$$H_{\text{MF}} = \sum_{0 < q \leq \pi} \sum_{y,y'} iA_{y,y'}(q) d_{q,y}^\dagger d_{q,y'}. \quad (6)$$

Thus, the problem reduces to diagonalizing the Hermitian matrix $iA(q)$ of dimension $L_y + 2$ whose components are given in the Supplemental Material [46]. The normal modes are given by $\gamma_{q,n}^\dagger = \sum_y U_{y,n}(q) d_{q,y}^\dagger$, where the unitary matrix $U(q)$ depends on χ_b and χ_c .

The mean-field parameters must be determined by self-consistency of the approximation. We obtain the self-consistency equations by calculating χ_b and χ_c as expectation values in the mean-field ground state, expressed in terms of the matrix elements $U_{y,n}(q)$. To account for the magnetic-field dependence of κ , we set $\kappa = h_x h_y h_z / J^2$. In addition, we parametrize the field direction by polar and azimuthal angles θ and ϕ with respect to the axes in Fig. 1(b). The mean-field parameters are then real functions of \tilde{J}/J , $|\mathbf{h}|/J$, θ and ϕ .

Our numerical results confirm that the mean-field parameters vanish below a critical coupling $\tilde{J}_c > 0$. In this case, the two sides of the line defect remain decoupled and the spectrum exhibits chiral Majorana modes with linear dispersion near $q = 0$. For $\tilde{J} > \tilde{J}_c$, we find that both χ_b and χ_c become nonzero with a continuous transition, in contrast with the first-order transition obtained by a variational analysis of the continuum model in Ref. [34]. As a check of our approach, we observe that $\chi_b \rightarrow 1$ in the limit $|h_z|/\tilde{J} \rightarrow 0$, as expected since $ib_j^z b_k^z$ in Eq. (3) become conserved \mathbb{Z}_2 operators when we neglect the Zeeman coupling. For nonzero χ_b and χ_c , the Majorana fermions on different sides hybridize and the 1D mode

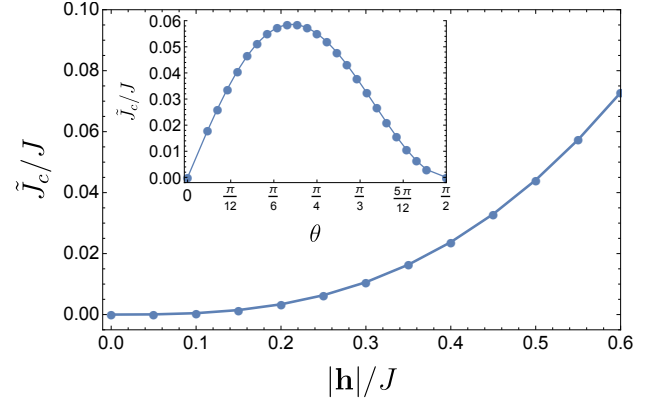


FIG. 3. Critical value of the interaction at the line defect as a function of the magnetic field. The field is fixed along the [111] direction ($\theta = \tan^{-1} \sqrt{2}$ and $\phi = \pi/4$). Inset: critical coupling as a function of θ for fixed $|\mathbf{h}| = 0.5J$ and $\phi = \pi/4$.

acquires a gap Δ_d . Figure 2 shows the gap for a magnetic field along the [111] direction. Interestingly, for a wide range of $\tilde{J} > \tilde{J}_c$ the gap Δ_d remains much smaller than the bulk gap $\Delta_b = 6\sqrt{3}\kappa$.

While the gap goes smoothly to zero at the transition, we can determine the critical point precisely by expanding the self-consistency equations for small values of the mean-field parameters. To first order in χ_b and χ_c , the equations take the form $\chi = \tilde{J}\Gamma\chi$, where $\chi = (\chi_b, \chi_c)^t$ and Γ is a 2×2 matrix easily computed in terms of the unitary matrix $U^{(0)}(q)$ that diagonalizes the mean-field Hamiltonian for $\chi_b = \chi_c = 0$ [46]. Requiring a nontrivial solution to the linear equation with $\tilde{J} \rightarrow \tilde{J}_c$, we obtain $\tilde{J}_c = 2(\text{tr } \Gamma)^{-1}[-w + \sqrt{w(w+1)}]$ with $w = (\text{tr } \Gamma)^2 / (4|\det \Gamma|)$. The dependence of \tilde{J}_c on the magnetic field is shown in Fig. 3. For fixed field direction, we observe a power-law behavior $\tilde{J}_c \sim |\mathbf{h}|^\beta$ with exponent $\beta \approx 3$. Moreover, the critical coupling varies with the field direction through the dependence on κ in the bulk and h_z at the line defect. Like the bulk gap, \tilde{J}_c vanishes when any of the components h_x , h_y or h_z go to zero. We have verified that the critical coupling also remains finite for in-plane fields, except for the special directions in which the bulk gap closes [46].

Low-energy effective theory.—For weak coupling $\tilde{J} < \tilde{J}_c$, the low-energy sector is described by two chiral Majorana fermions, each associated with one side of the line defect. To derive the effective field theory, we expand the matrix $A(q)$ in Eq. (6) to first order in q . The bound state wave functions decay exponentially with the distance from the defect and can be determined exactly for $q \rightarrow 0$. Solving the eigenvalue equation with dispersion $\varepsilon_{R/L}(q) = \pm vq$ for the chiral modes, we find an analytical expression for the velocity [46]

$$v = \frac{|\kappa|h_z^2}{J^2 + h_z^2/3}. \quad (7)$$

Note that the velocity vanishes when $h_z \rightarrow 0$ or $\kappa \rightarrow 0$.

The low-energy Hamiltonian is effectively 1D:

$$H_{\text{low}} = \sum_{q>0} vq \left(\gamma_{qR}^\dagger \gamma_{qR} - \gamma_{qL}^\dagger \gamma_{qL} \right), \quad (8)$$

where $\gamma_{q\alpha}$, with $\alpha = R, L$, are the annihilation operators for right and left movers. In the continuum limit, the chiral Majorana fermions are $\gamma_\alpha(x) = \sqrt{2/L_x} \sum_{q>0} (e^{iqx} \gamma_{q\alpha} + e^{-iqx} \gamma_{q\alpha}^\dagger)$. We can then write

$$H_{\text{low}} = \frac{1}{4} \int dx \left[\gamma_R (-iv \partial_x) \gamma_R + \gamma_L (iv \partial_x) \gamma_L \right]. \quad (9)$$

Next, we calculate the representation of the spin operator in the low-energy theory in terms of the chiral Majorana fermions. For the geometry in Fig. 1(a), only the σ_j^z component for sites j near the line defect has a nonzero projection onto the gapless modes. Expanding c_j and b_j^z on a defect site in terms of the normal modes to first order in q , we obtain

$$S_j^z = \frac{1}{2} \sigma_j^z \sim S_\alpha^z(x) = \frac{i\alpha s}{2} \gamma_\alpha(x) \partial_x \gamma_\alpha(x), \quad (10)$$

where $s = J^2 |\kappa| h_z / (J^2 + h_z^2/3)^2$ and we select $\alpha = R, L = +, -$ according to the chiral mode whose wave function lies on the same side as site j . The representation in Eq. (10) could be argued on symmetry grounds [34]. We stress that, in contrast with the usual parton representation using complex Abrikosov fermions $\mathbf{S}_j = \frac{1}{2} f_a^\dagger \boldsymbol{\sigma}_{ab} f_b$ [2, 47], the Majorana fermion representation requires a spatial derivative, which increases the scaling dimension of the operator in Eq. (10).

The projection of the quartic term in Eq. (3) onto the gapless modes yields $V \sim g \int dx \gamma_R \partial_x \gamma_R \gamma_L \partial_x \gamma_L$ with $g \sim \tilde{J} s^2$. This irrelevant interaction is the leading perturbation to the low-energy fixed-point Hamiltonian [34, 35]. Crucially, the mass term $im \gamma_R \gamma_L$ is forbidden, as local operators must be bilinears of the emergent Majorana fermions on the same side of the line defect. As long as $v > 0$, the transition occurs at a finite critical coupling, spontaneously breaking the $\mathbb{Z}_2 \times \mathbb{Z}_2$ symmetry of independently flipping the signs of γ_R and γ_L . Beyond the mean-field level, the critical point is described by the tricritical Ising conformal field theory [35].

NMR response.—The effective field theory allows us to calculate the spin-lattice relaxation rate at low temperatures for a nuclear spin adjacent to the line defect. When restricted to the contribution from the gapless 1D mode, the linear response formula for T_1^{-1} becomes [48, 49]

$$\frac{1}{T_1} = \frac{\gamma_N^2}{2L_x} \sum_q |A_{\text{hf}}(q)|^2 S(q, \omega_0), \quad (11)$$

where γ_N is the nuclear gyromagnetic ratio for ^{35}Cl NMR in $\alpha\text{-RuCl}_3$ [36–39], $A_{\text{hf}}(q)$ is the hyperfine coupling form

factor, $\omega_0 = \gamma_N |\mathbf{h}|$ is the Larmor nuclear resonance frequency, and

$$S(q, \omega_0) = \int dx dt e^{i(\omega_0 t - qx)} \langle \tilde{S}_\alpha^+(x, t) \tilde{S}_\alpha^-(0, 0) \rangle \quad (12)$$

is the transverse dynamical spin structure factor at temperature T for either value of α . Here $\tilde{S}^\pm(x, t) = \tilde{S}^x(x, t) \pm i \tilde{S}^y(x, t)$ are time-evolved ladder operators that perform spin flips with respect to the magnetic-field axis. On the other hand, the spin components S^γ were originally defined with respect to the axes in Fig. 1(b). Rotating the coordinate system, we obtain

$$\begin{aligned} \tilde{S}^\pm &= -S^z \sin \theta + S^x (\cos \theta \cos \phi \mp i \sin \phi) \\ &\quad + S^y (\cos \theta \cos \phi \pm i \sin \phi). \end{aligned} \quad (13)$$

Since only the S^z operator has a nonzero projection onto the gapless modes, we have $\langle \tilde{S}_\alpha^+(x, t) \tilde{S}_\alpha^-(0, 0) \rangle = \langle S_\alpha^z(x, t) S_\alpha^z(0, 0) \rangle \sin^2 \theta$, with $S_\alpha^z(x)$ given by Eq. (10).

We calculate T_1^{-1} using Green's functions for noninteracting Majorana fermions described by the Hamiltonian in Eq. (9). The experimentally relevant regime with $T \sim 1$ K and $\omega_0 \sim 10$ MHz is $\omega_0 \ll T$, where we set $\hbar = k_B = 1$. In this regime, the dynamical structure factor can be written as $S(q, \omega_0) \approx -(2T/\omega_0) \text{Im} \chi^{\text{ret}}(q, \omega_0)$, where $\chi^{\text{ret}}(q, \omega_0)$ is the retarded dynamical susceptibility for the $S_\alpha^z(x)$ operator. The latter can be calculated by analytical continuation of the Matsubara correlation function [46]. We find

$$\frac{1}{T_1} \approx \frac{\pi^2 s^2 \gamma_N^2}{6v^4} |A_{\text{hf}}(0)|^2 \sin^2 \theta T^3. \quad (14)$$

This result is valid for $T \lesssim v$, since v sets the high-energy cutoff of the effective field theory when the lattice parameter is set to unity. Note that the temperature window shrinks to zero for $\kappa \rightarrow 0$.

A cubic temperature dependence in the spin-lattice relaxation rate has been observed experimentally [36] and interpreted as evidence for a gapless spin liquid in $\alpha\text{-RuCl}_3$. Indeed, $T_1^{-1} \sim T^3$ is expected for a generic Kitaev spin liquid with a massless Dirac spectrum [50], possible when the magnetic field points along the particular directions in which $\kappa = 0$. However, the results of Ref. [36] showed a cubic temperature dependence over a broad field range, independent of orientation. For magnetic fields above 12 T, the spin-lattice relaxation rate decays faster with decreasing temperature. The deviation from the T^3 behavior at high fields indicates a suppression of the mechanism responsible for the gapless modes, as expected when the material enters the trivial polarized phase. Meanwhile, other measurements of $1/T_1$ in $\alpha\text{-RuCl}_3$ favor a picture of fully gapped spin excitations [38, 39].

Here we suggest that the apparently gapless behavior may have its origin in 1D modes bound to line defects.

Importantly, the effective field theory shows that the robustness of these gapless modes is a *universal* property of the non-Abelian Kitaev spin liquid. While the realistic spin model for α -RuCl₃ must include Heisenberg and off-diagonal exchange interactions [7] neglected in Eq. (1), our main conclusions do not depend on microscopic details. As long as the perturbations to the Kitaev model do not destroy the topological order, they can only renormalize the prefactor of $1/T_1$ in Eq. (14). The T^3 dependence only relies on the existence of chiral Majorana modes with linear dispersion. In fact, the exponent can be traced back to the scaling dimension of the spin operator in Eq. (10). By contrast, for a 1D system of complex fermions described by Luttinger liquid theory, the small- q contribution to the spin-lattice relaxation rate scales as $T_1^{-1} \sim T$ [49, 51]. Thus, our result does not follow from a usual density-of-states factor, but is connected with the Majorana fermion nature of the elementary excitations. We note that other types of defects in the Kitaev spin liquid, such as site dilution, can also give rise to a power-law dependence in T_1^{-1} , but with lower exponents [25].

Our results also reveal a characteristic dependence on the magnetic-field direction. However, the geometric factor $\sin^2 \theta$ holds only for a line defect running between zigzag edges. For more general geometries, different spin components may have projections onto the chiral Majorana modes, modifying this geometric factor. For randomly oriented line defects, the angular dependence averages out, which is consistent with the experiment of Ref. [36]. An alternative explanation, put forward in Ref. [52], is that the intermediate phase of α -RuCl₃ might be described by a U(1) spin liquid whose gap remains small, below the measurement temperature, for arbitrary field directions. While the nature of this phase is under scrutiny again [53], our proposal highlights the role of line defects when unraveling the properties of Kitaev materials. To distinguish between different scenarios for the gapless behavior, it would be interesting to single out the contribution from line defects by controlling their density and orientation [28] in different samples.

Conclusions.— We showed that gapless Majorana modes bound to line defects can survive in the bulk of non-Abelian Kitaev spin liquids, with clear signatures in low-energy properties. As an example, we showed that these modes give rise to a cubic temperature dependence of the spin-lattice relaxation rate, offering an explanation for the experimental findings of Ref. [36]. The critical value of the interaction below which the 1D modes remain gapless can be tuned by the magnitude and orientation of the external magnetic field.

We thank R. Egger and E. Miranda for helpful discussions. We acknowledge funding by Brazilian agencies CAPES (L.R.D.F.) and CNPq (R.G.P.). Research at IIP-UFRN is supported by Brazilian ministries MEC and MCTI. This work was also supported by a grant from Associação Instituto Internacional de Física.

-
- [1] A. Kitaev, *Ann. Phys.* **321**, 2 (2006).
 - [2] L. Savary and L. Balents, *Rep. Prog. Phys.* **80**, 016502 (2016).
 - [3] J. Knolle and R. Moessner, *Annu. Rev. Condens. Matter Phys.* **10**, 451 (2019).
 - [4] C. Broholm, R. J. Cava, S. A. Kivelson, D. G. Nocera, M. R. Norman, and T. Senthil, *Science* **367**, eaay0668 (2020).
 - [5] G. Jackeli and G. Khaliullin, *Phys. Rev. Lett.* **102**, 017205 (2009).
 - [6] J. c. v. Chaloupka, G. Jackeli, and G. Khaliullin, *Phys. Rev. Lett.* **105**, 027204 (2010).
 - [7] J. G. Rau, E. K.-H. Lee, and H.-Y. Kee, *Phys. Rev. Lett.* **112**, 077204 (2014).
 - [8] Y. Singh, S. Manni, J. Reuther, T. Berlijn, R. Thomale, W. Ku, S. Trebst, and P. Gegenwart, *Phys. Rev. Lett.* **108**, 127203 (2012).
 - [9] S. Hwan Chun, J.-W. Kim, J. Kim, H. Zheng, C. C. Stoumpos, C. D. Malliakas, J. F. Mitchell, K. Mehlawat, Y. Singh, Y. Choi, T. Gog, A. Al-Zein, M. M. Sala, M. Krisch, J. Chaloupka, G. Jackeli, G. Khaliullin, and B. J. Kim, *Nat. Phys.* **11**, 462 (2015).
 - [10] K. Kitagawa, T. Takayama, Y. Matsumoto, A. Kato, R. Takano, Y. Kishimoto, S. Bette, R. Dinnebier, G. Jackeli, and H. Takagi, *Nature* **554**, 341 (2018).
 - [11] K. W. Plumb, J. P. Clancy, L. J. Sandilands, V. V. Shankar, Y. F. Hu, K. S. Burch, H.-Y. Kee, and Y.-J. Kim, *Phys. Rev. B* **90**, 041112(R) (2014).
 - [12] H.-S. Kim, V. S. V., A. Catuneanu, and H.-Y. Kee, *Phys. Rev. B* **91**, 241110(R) (2015).
 - [13] A. Banerjee, C. A. Bridges, J.-Q. Yan, A. A. Aczel, L. Li, M. B. Stone, G. E. Granroth, M. D. Lumsden, Y. Yiu, J. Knolle, S. Bhattacharjee, D. L. Kovrizhin, R. Moessner, D. A. Tennant, D. G. Mandrus, and S. E. Nagler, *Nat. Mater.* **15**, 733 (2016).
 - [14] R. Hentrich, X. Hong, M. Gillig, F. Caglieris, M. Čulo, M. Shahrokhtvand, U. Zeitler, M. Roslova, A. Isaeva, T. Doert, L. Janssen, M. Vojta, B. Büchner, and C. Hess, *Phys. Rev. B* **102**, 235155 (2020).
 - [15] A. Banerjee, P. Lampen-Kelley, J. Knolle, C. Balz, A. A. Aczel, B. Winn, Y. Liu, D. Pajerowski, J. Yan, C. A. Bridges, A. T. Savici, B. C. Chakoumakos, M. D. Lumsden, D. A. Tennant, R. Moessner, D. G. Mandrus, and S. E. Nagler, *npj Quantum Materials* **3**, 8 (2018).
 - [16] Y. Kasahara, T. Ohnishi, Y. Mizukami, O. Tanaka, S. Ma, K. Sugii, N. Kurita, H. Tanaka, J. Nasu, Y. Motome, and et al., *Nature* **559**, 227 (2018).
 - [17] T. Yokoi, S. Ma, Y. Kasahara, S. Kasahara, T. Shibauchi, N. Kurita, H. Tanaka, J. Nasu, Y. Motome, C. Hickey, S. Trebst, and Y. Matsuda, *Science* **373**, 568 (2021).
 - [18] O. Tanaka, Y. Mizukami, R. Harasawa, K. Hashimoto, N. Kurita, H. Tanaka, S. Fujimoto, Y. Matsuda, E. G. Moon, and T. Shibauchi, “Thermodynamic evidence for field-angle dependent Majorana gap in a Kitaev spin liquid,” (2020), [arXiv:2007.06757 \[cond-mat.str-el\]](https://arxiv.org/abs/2007.06757).
 - [19] A. J. Willans, J. T. Chalker, and R. Moessner, *Phys. Rev. Lett.* **104**, 237203 (2010).
 - [20] M. Vojta, A. K. Mitchell, and F. Zschöcke, *Phys. Rev. Lett.* **117**, 037202 (2016).
 - [21] J. Knolle, R. Moessner, and N. B. Perkins, *Phys. Rev. Lett.* **122**, 047202 (2019).

- [22] M. G. Yamada, *npj Quantum Materials* **5**, 82 (2020).
- [23] E. C. Andrade, L. Janssen, and M. Vojta, *Phys. Rev. B* **102**, 115160 (2020).
- [24] W.-H. Kao, J. Knolle, G. B. Halász, R. Moessner, and N. B. Perkins, *Phys. Rev. X* **11**, 011034 (2021).
- [25] J. Nasu and Y. Motome, *Phys. Rev. B* **104**, 035116 (2021).
- [26] J. Sólyom, *Fundamentals of the Physics of Solids: Volume 1: Structure and Dynamics* (Springer Berlin Heidelberg, 2007).
- [27] Z. Lin, B. R. Carvalho, E. Kahn, R. Lv, R. Rao, H. Terrones, M. A. Pimenta, and M. Terrones, *2D Materials* **3**, 022002 (2016).
- [28] H.-P. Komsa, S. Kurasch, O. Lehtinen, U. Kaiser, and A. V. Krasheninnikov, *Phys. Rev. B* **88**, 035301 (2013).
- [29] R. D. Johnson, S. C. Williams, A. A. Haghighirad, J. Singleton, V. Zapf, P. Manuel, I. I. Mazin, Y. Li, H. O. Jeschke, R. Valentí, and R. Coldea, *Phys. Rev. B* **92**, 235119 (2015).
- [30] H.-S. Kim and H.-Y. Kee, *Phys. Rev. B* **93**, 155143 (2016).
- [31] H. B. Cao, A. Banerjee, J.-Q. Yan, C. A. Bridges, M. D. Lumsden, D. G. Mandrus, D. A. Tennant, B. C. Chakoumakos, and S. E. Nagler, *Phys. Rev. B* **93**, 134423 (2016).
- [32] O. Petrova, P. Mellado, and O. Tchernyshyov, *Phys. Rev. B* **88**, 140405(R) (2013).
- [33] O. Petrova, P. Mellado, and O. Tchernyshyov, *Phys. Rev. B* **90**, 134404 (2014).
- [34] D. Aasen, R. S. K. Mong, B. M. Hunt, D. Mandrus, and J. Alicea, *Phys. Rev. X* **10**, 031014 (2020).
- [35] A. Rahmani, X. Zhu, M. Franz, and I. Affleck, *Phys. Rev. Lett.* **115**, 166401 (2015).
- [36] J. Zheng, K. Ran, T. Li, J. Wang, P. Wang, B. Liu, Z.-X. Liu, B. Normand, J. Wen, and W. Yu, *Phys. Rev. Lett.* **119**, 227208 (2017).
- [37] S.-H. Baek, S.-H. Do, K.-Y. Choi, Y. S. Kwon, A. U. B. Wolter, S. Nishimoto, J. van den Brink, and B. Büchner, *Phys. Rev. Lett.* **119**, 037201 (2017).
- [38] N. Janša, A. Zorko, M. Gomilšek, M. Pregelj, K. W. Krämer, D. Biner, A. Biffin, C. Rüegg, and M. Klanjšek, *Nat. Phys.* **14**, 786 (2018).
- [39] Y. Nagai, T. Jinno, J. Yoshitake, J. Nasu, Y. Motome, M. Itoh, and Y. Shimizu, *Phys. Rev. B* **101**, 020414(R) (2020).
- [40] S. M. Winter, A. A. Tsirlin, M. Daghofer, J. van den Brink, Y. Singh, P. Gegenwart, and R. Valentí, *J. Phys.: Condens. Matter* **29**, 493002 (2017).
- [41] H. Takagi, T. Takayama, G. Jackeli, G. Khaliullin, and S. E. Nagler, *Nat. Rev. Phys.* **1**, 264 (2019).
- [42] R. Yadav, S. Rachel, L. Hozoi, J. van den Brink, and G. Jackeli, *Phys. Rev. B* **98**, 121107(R) (2018).
- [43] J. S. Gordon, A. Catuneanu, E. S. Sørensen, and H.-Y. Kee, *Nat. Comm.* **10**, 2470 (2019).
- [44] J. Nasu, Y. Kato, Y. Kamiya, and Y. Motome, *Phys. Rev. B* **98**, 060416(R) (2018).
- [45] J. Knolle, S. Bhattacharjee, and R. Moessner, *Phys. Rev. B* **97**, 134432 (2018).
- [46] See the Online Supplemental Material for more information on the self-consistent mean-field approach and the calculation of the spin-lattice relaxation rate using the Majorana fermion Green's function.
- [47] X. Wen, *Quantum Field Theory of Many-Body Systems* (Oxford University Press, Oxford, 2004).
- [48] P. Carretta and A. Keren, in *Introduction to Frustrated Magnetism: Materials, Experiments, Theory*, edited by C. Lacroix, P. Mendels, and F. Mila (Springer, Berlin, Heidelberg, 2011).
- [49] J. Sirker, R. G. Pereira, and I. Affleck, *Phys. Rev. B* **83**, 035115 (2011).
- [50] X.-Y. Song, Y.-Z. You, and L. Balents, *Phys. Rev. Lett.* **117**, 037209 (2016).
- [51] S. Sachdev, *Phys. Rev. B* **50**, 13006 (1994).
- [52] Z.-X. Liu and B. Normand, *Phys. Rev. Lett.* **120**, 187201 (2018).
- [53] P. Czajka, T. Gao, M. Hirschberger, P. Lampen-Kelley, A. Banerjee, J. Yan, D. G. Mandrus, S. E. Nagler, and N. P. Ong, *Nat. Phys.* **17**, 915 (2021).

Supplemental Material: Gapless excitations in non-Abelian Kitaev spin liquids with line defects

1. Self-consistent mean-field approach

In the mean-field Hamiltonian written in Eq. (6) of the main text, the Hermitean matrix of dimension $L_y + 2$ is

$$iA(q) = \begin{pmatrix} 0 & i\gamma & 0 & 0 & 0 & 0 & 0 & 0 & 0 & i\tilde{J}\chi_c \\ -i\gamma & \alpha & is & -\beta & 0 & 0 & 0 & 0 & i\tilde{J}\chi_b & 0 \\ 0 & -is & -\alpha & ir & \beta & 0 & 0 & 0 & 0 & 0 \\ 0 & -\beta & ir & \alpha & is & -\beta & 0 & 0 & 0 & 0 \\ 0 & 0 & \beta & -is & -\alpha & ir & \beta & 0 & 0 & 0 \\ 0 & 0 & 0 & \ddots & \ddots & \ddots & \ddots & \ddots & 0 & 0 \\ 0 & 0 & 0 & 0 & \ddots & \ddots & \ddots & \ddots & \ddots & 0 \\ 0 & 0 & 0 & 0 & 0 & -\beta & -ir & \alpha & is & 0 \\ 0 & -i\tilde{J}\chi_b & 0 & 0 & 0 & 0 & \beta & -is & -\alpha & -i\gamma \\ -i\tilde{J}\chi_c & 0 & 0 & 0 & 0 & 0 & 0 & 0 & i\gamma & 0 \end{pmatrix}, \quad (15)$$

with matrix elements as in Ref. [1]:

$$\alpha = 2\kappa \sin(q), \quad (16)$$

$$\beta = 2\kappa \sin(q/2), \quad (17)$$

$$r = J, \quad (18)$$

$$s = -2J \cos(q/2), \quad (19)$$

$$\gamma = -h_z. \quad (20)$$

The mean-field parameters can be written as

$$\chi_b = \langle id_{x,0} d_{x,L_y+1} \rangle, \quad (21)$$

$$\chi_c = \langle id_{x,1} d_{x,L_y} \rangle, \quad (22)$$

where the expectation values are calculated in the mean-field ground state.

Performing a unitary transformation

$$d_{q,y} = \sum_{n=1}^{L_y+2} U_{y,n}(q) \gamma_{q,n}, \quad (23)$$

we diagonalize the mean-field Hamiltonian in the form

$$H_{\text{MF}} = \sum_{0 < q \leq \pi} \sum_{n=1}^{L_y+2} \varepsilon_n(q) \gamma_{q,n}^\dagger \gamma_{q,n}. \quad (24)$$

The eigenvalues are sorted such that $\varepsilon_{n+\frac{L_y}{2}}(q) = -\varepsilon_n(q) \leq 0$, for $1 \leq n \leq \frac{L_y}{2} + 1$. The mean-field ground state is a Dirac sea in which all negative-energy states are occupied, so that $\langle \gamma_{q,n}^\dagger \gamma_{q',n'} \rangle = \delta_{qq'} \delta_{nn'} \Theta(-\varepsilon_n(q))$. As a result, we can express the mean-field parameters in terms of the matrix elements $U_{y,n}(q)$ as follows:

$$\chi_b = \frac{4}{L_x} \sum_{0 < q \leq \pi} \sum_{n=1}^{\frac{L_y}{2}+1} \text{Im} [U_{0,n}^*(q) U_{L_y+1,n}(q)], \quad (25)$$

$$\chi_c = \frac{4}{L_x} \sum_{0 < q \leq \pi} \sum_{n=1}^{\frac{L_y}{2}+1} \text{Im} [U_{1,n}^*(q) U_{L_y,n}(q)]. \quad (26)$$

In Fig. 4, we show the result for the mean-field parameters obtained by numerically iterating Eqs. (25) and (26). Note that χ_b and χ_c vanish below the critical coupling \tilde{J}_c . Moreover, for a fixed value of $|\mathbf{h}|$, the critical coupling for an in-plane field along the a axis is slightly larger than for a field perpendicular to the ab plane.

2. Determining the critical coupling

Here we will use perturbation theory for small values of the mean-field parameters to calculate precisely the critical coupling \tilde{J}_c . Let $\{\phi_n(q)\}$ be the eigenvectors of $A(q)$, represented as column vectors and corresponding to the columns of the matrix $U_{y,n}(q)$. These vectors satisfy the eigenvalue equation

$$iA(q)\phi_n(q) = \varepsilon_n(q)\phi_n(q). \quad (27)$$

Close to the critical point, we may expand this equation linearly in χ_b and χ_c , which appear in $A(q)$ multiplying \tilde{J} . We define the coefficients of the expansion as

$$\phi_n(q) = \phi_n^{(0)}(q) + \tilde{J} \chi_b \phi_n^{(1b)}(q) + \tilde{J} \chi_c \phi_n^{(1c)}(q) + \dots, \quad (28)$$

$$\varepsilon_n(q) = \varepsilon_n^{(0)}(q) + \tilde{J} \chi_b \varepsilon_n^{(1b)}(q) + \tilde{J} \chi_c \varepsilon_n^{(1c)}(q) + \dots, \quad (29)$$

$$iA(q) = iA^{(0)}(q) + \tilde{J} \chi_b \mathcal{V}_b + \tilde{J} \chi_c \mathcal{V}_c + \dots, \quad (30)$$

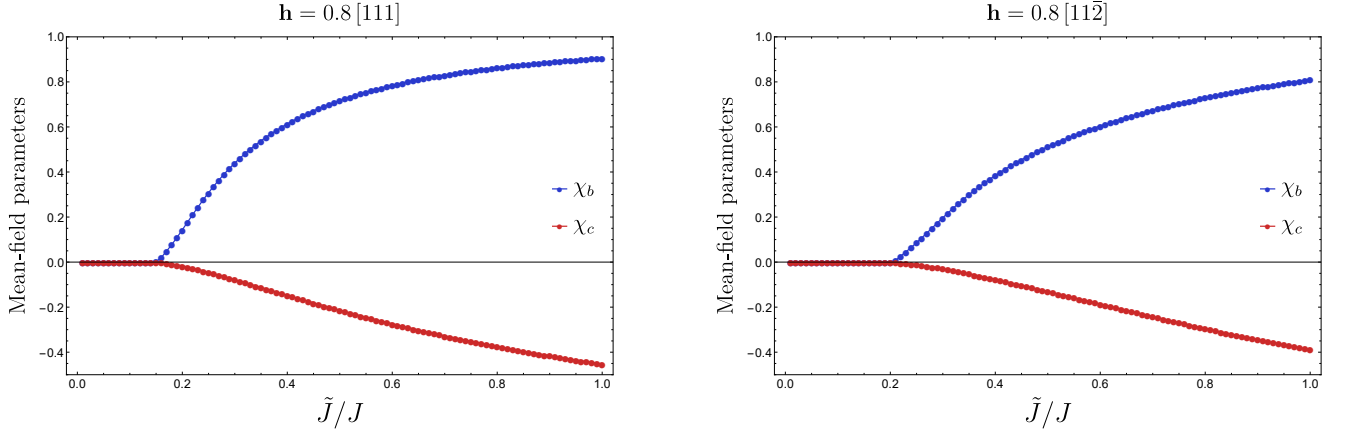


FIG. 4. Mean-field parameters for a magnetic field with $|\mathbf{h}| = 0.8J$ and two representative directions. Left: magnetic field in the $[111]$ direction, perpendicular to the ab plane which contains the honeycomb lattice. Right: in-plane field in the $[11\bar{2}]$ direction, usually denoted as the a axis.

where the matrices are

$$\mathcal{V}_b = i \begin{pmatrix} 0 & 0 & 0 & 0 & 0 & 0 \\ 0 & 0 & 0 & 0 & 1 & 0 \\ 0 & \ddots & \ddots & \ddots & 0 & 0 \\ 0 & 0 & \ddots & \ddots & \ddots & 0 \\ 0 & -1 & 0 & 0 & 0 & 0 \\ 0 & 0 & 0 & 0 & 0 & 0 \end{pmatrix}, \quad \mathcal{V}_c = i \begin{pmatrix} 0 & 0 & 0 & 0 & 0 & 1 \\ 0 & 0 & 0 & 0 & 0 & 0 \\ 0 & \ddots & \ddots & \ddots & 0 & 0 \\ 0 & 0 & \ddots & \ddots & \ddots & 0 \\ 0 & 0 & 0 & 0 & 0 & 0 \\ -1 & 0 & 0 & 0 & 0 & 0 \end{pmatrix}. \quad (31)$$

The coefficients in the first-order correction to the energies can be calculated as

$$\varepsilon_n^{(1b)}(q) = [\phi_n^{(0)}(q)]^t \mathcal{V}_b \phi_n^{(0)}(q), \quad \varepsilon_n^{(1c)}(q) = [\phi_n^{(0)}(q)]^t \mathcal{V}_c \phi_n^{(0)}(q). \quad (32)$$

The unperturbed eigenvectors $\phi_n^{(0)}(q)$ are given by the column vectors of the matrix $U^{(0)}(q)$, which we obtain numerically by diagonalizing the Hamiltonian with $\tilde{J} = 0$. To first order in χ_b and χ_c , we obtain

$$U_{y,n}(q) = U_{y,n}^{(0)}(q) + \tilde{J} \sum_{n' \neq n} \left\{ \chi_b \frac{[\phi_n^{(0)}(q)]^t \mathcal{V}_b \phi_{n'}^{(0)}(q)}{\varepsilon_n^{(0)}(q) - \varepsilon_{n'}^{(0)}(q)} + \chi_c \frac{[\phi_n^{(0)}(q)]^t \mathcal{V}_c \phi_{n'}^{(0)}(q)}{\varepsilon_n^{(0)}(q) - \varepsilon_{n'}^{(0)}(q)} \right\} U_{y,n'}^{(0)}(q). \quad (33)$$

Equations (25) and (26) involve the imaginary part of the product $U_{y,n}^*(q) U_{y',n}(q)$. The latter vanishes to zeroth order in mean-field parameters. Expanding to first order, we obtain the linear equations

$$\begin{pmatrix} \chi_b \\ \chi_c \end{pmatrix} = \tilde{J} \begin{pmatrix} \Gamma^{bb} & \Gamma^{bc} \\ \Gamma^{cb} & \Gamma^{cc} \end{pmatrix} \begin{pmatrix} \chi_b \\ \chi_c \end{pmatrix} + \dots, \quad (34)$$

with coefficients

$$\Gamma^{bb} = \Gamma^{cc} = \frac{4}{L_x} \text{Re} \left[\sum_{0 < q \leq \pi} \sum_{n, n'}' \frac{1}{\varepsilon_n^{(0)} - \varepsilon_{n'}^{(0)}} \left(U_{1,n}^{(0)*} U_{L_y, n'}^{(0)} - U_{1, n'}^{(0)} U_{L_y, n}^{(0)*} \right) \left(U_{0,n}^{(0)*} U_{L_y+1, n'}^{(0)} - U_{0, n'}^{(0)} U_{L_y+1, n}^{(0)*} \right) \right], \quad (35)$$

$$\Gamma^{bc} = -\frac{4}{L_x} \sum_{0 < q \leq \pi} \sum_{n, n'}' \frac{1}{\varepsilon_n^{(0)} - \varepsilon_{n'}^{(0)}} \left| U_{0,n}^{(0)*} U_{L_y+1, n'}^{(0)} - U_{0, n'}^{(0)} U_{L_y+1, n}^{(0)*} \right|^2, \quad (36)$$

$$\Gamma^{cb} = -\frac{4}{L_x} \sum_{0 < q \leq \pi} \sum_{n, n'}' \frac{1}{\varepsilon_n^{(0)} - \varepsilon_{n'}^{(0)}} \left| U_{1,n}^{(0)*} U_{L_y, n'}^{(0)} - U_{1, n'}^{(0)} U_{L_y, n}^{(0)*} \right|^2, \quad (37)$$

where the sum $\sum'_{n,n'}$ runs for $1 \leq n \leq L_y/2 + 1$ and $n' \neq n$.

Equation (34) becomes exact in the limit $\tilde{J} \rightarrow \tilde{J}_c^+$. A nontrivial solution with $\chi_b \neq 0$ and $\chi_c \neq 0$ requires

$$\tilde{J}_c^2 \det \Gamma - \tilde{J}_c \text{tr} \Gamma + 1 = 0, \quad (38)$$

where $\det \Gamma = (\Gamma^{bb})^2 - \Gamma^{bc}\Gamma^{cb}$ and $\text{tr} \Gamma = 2\Gamma^{bb}$. From the general structure of the matrix elements of Γ and using the Cauchy-Schwarz inequality, we can show that $\det \Gamma < 0$. We found numerically that $\text{tr} \Gamma > 0$ for $J > 0$. Thus, the only positive solution is

$$\tilde{J}_c = \frac{\text{tr} \Gamma}{2|\det \Gamma|} \left[-1 + \sqrt{1 + \frac{4|\det \Gamma|}{(\text{tr} \Gamma)^2}} \right]. \quad (39)$$

3. Continuum limit of Hamiltonian and spin operators

The uncoupled phase is described by the mean-field Hamiltonian with $\chi_b = \chi_c = 0$. Equivalently, we can set $\tilde{J} = 0$ in Eq. (15). For $\kappa \neq 0$, there are two gapless modes with linear dispersion about $q = 0$ and all other modes are gapped.

To describe the low-energy physics, we treat q as a small parameter and expand the Hamiltonian matrix as

$$iA(q) = \mathcal{H}^{(0)} + q\mathcal{H}^{(1)} + \dots \quad (40)$$

The matrix $\mathcal{H}^{(0)}$ is tridiagonal with coefficients depending on h_z and J , whereas $\mathcal{H}^{(1)}$ is a pentadiagonal matrix with a linear dependence on κ .

We denote the two eigenvectors of $iA(q)$ associated with the gapless modes by $\phi_R(q)$ and $\phi_L(q)$. When we project onto these low-energy modes, Eq. (23) reduces to

$$d_{q,y} \sim \phi_{R,y}(q)\gamma_{q,R} + \phi_{L,y}(q)\gamma_{q,L}. \quad (41)$$

We expand the eigenvectors linearly in momentum as

$$\phi_{R/L}(q) = \phi_{R/L}^{(0)} + q\phi_{R/L}^{(1)} + \dots \quad (42)$$

For $q \rightarrow 0$, these vectors become the two eigenvectors of $\mathcal{H}^{(0)}$ with zero eigenvalue. Consider L_y even and $L_y \gg 1$. For $\kappa > 0$, the non-zero components of these vectors are

$$\phi_{L,y}^{(0)} = \frac{h_z}{2J} (-1)^{\frac{y}{2}} e^{-\frac{L_y-1-y}{\xi}} \phi_{L,L_y+1}^{(0)}, \quad y \text{ odd}, y \leq L_y - 1, \quad (43)$$

$$\phi_{R,y}^{(0)} = \frac{h_z}{2J} (-1)^{\frac{y}{2}} e^{-\frac{y-2}{\xi}} \phi_{R,0}^{(0)}, \quad y \text{ even}, y \geq 2, \quad (44)$$

where the correlation length is $\xi = 2/\ln 2$ and the normalization factor is $\phi_{L,L_y+1}^{(0)} = \phi_{R,0}^{(0)} = -J(J^2 + h_z^2/3)^{-1/2}$. The right- and left-moving modes are related by a transformation that takes $y \mapsto L_y + 1 - y$ and $v \mapsto -v$.

The eigenvalue equation at first order in q yields

$$\mathcal{H}^{(0)}\phi_\alpha^{(1)} + \mathcal{H}^{(1)}\phi_\alpha^{(0)} = \alpha v \phi_\alpha^{(0)}, \quad (45)$$

where $\alpha = R/L = \pm$. Using that $\phi_\alpha^{(0)}$ has eigenvalue zero in $\mathcal{H}^{(0)}$, we obtain

$$v = [\phi_R^{(0)}]^\dagger \mathcal{H}^{(1)} \phi_R^{(0)} = \frac{|\kappa|h_z^2}{J^2 + h_z^2/3}. \quad (46)$$

Here the velocity is positive by definition. For $\kappa > 0$, the right movers are localized at the ℓ_1 edge ($y = 1$) and the left movers at the ℓ_2 edge ($y = L_y$). If we vary the magnetic field so that κ changes sign, the Chern number in the bulk also changes sign and the chirality at the edge is reversed, and we must relabel $R \leftrightarrow L$ in Eqs. (43) and (44).

For $\kappa > 0$, the spin operator at edges ℓ_1 and ℓ_2 are

$$S_R^z(x) = \frac{i}{2} d_{x,0} d_{x,1} = \frac{i}{L_x} \sum_{-\pi < q, k \leq \pi} e^{i(q+k)x} d_{q,0} d_{k,1} \quad (47)$$

$$S_L^z(x) = \frac{i}{2} d_{x,L_y+1} d_{x,L_y} = \frac{i}{L_x} \sum_{-\pi < q, k \leq \pi} e^{i(q+k)x} d_{q,L_y+1} d_{k,L_y}. \quad (48)$$

Substituting the projected mode expansion in Eq. (41), we find that the term of zeroth order in q vanishes, and we need to consider the first-order corrections. As the first and last rows of $\mathcal{H}^{(1)}$ are zero, the first and last components of Eq. (45) yield a simple relation between the required components of $\phi_\alpha^{(0)}$ and $\phi_\alpha^{(1)}$. We find

$$\phi_{R,1}^{(1)} = \frac{v}{-ih_z} \phi_{R,0}^{(0)} = \frac{Jv}{ih_z} (J^2 + h_z^2/3)^{-1/2}, \quad (49)$$

$$\phi_{L,L_y}^{(1)} = \frac{-v}{-ih_z} \phi_{L,L_y+1}^{(0)} = -\frac{Jv}{ih_z} (J^2 + h_z^2/3)^{-1/2}. \quad (50)$$

Using Eq. (41) and fact that the low-energy modes are localized at the edge, we can write the spin operators as

$$S_R^z(x) = \frac{i}{L_x} \sum_{q,k} e^{i(q+k)x} \phi_{R,0}(q) \phi_{R,1}(q) \gamma_{q,R} \gamma_{k,R}, \quad (51)$$

$$S_L^z(x) = \frac{i}{L_x} \sum_{q,k} e^{i(q+k)x} \phi_{L,L_y+1}(q) \phi_{R,L_y}(q) \gamma_{q,L} \gamma_{k,L}. \quad (52)$$

The coefficients up to linear order in q are

$$\phi_{R,0}(q) \phi_{R,1}(q) = -\phi_{L,L_y+1}(q) \phi_{R,L_y}(q) = q \frac{iJ^2v}{h_z} \left(J^2 + \frac{h_z^2}{3} \right)^{-1} \equiv isq. \quad (53)$$

Taking the Fourier transform back to real space in the continuum, we can write $S_\alpha^z(x)$ in terms of the chiral Majorana fermions $\gamma_\alpha(x)$ as in Eq. (10) of the main text.

4. Calculation of dynamic spin correlations at finite temperature

Consider the spin-spin correlation in imaginary time:

$$\tilde{\chi}_\alpha(x - x', \tau) = -\langle T_\tau S_\alpha^z(x, \tau) S_\alpha^z(x', 0) \rangle_\beta = \frac{s^2}{4} \left\langle T_\tau \gamma_\alpha(x, \tau) \partial_x \gamma_\alpha(x, \tau) \gamma_\alpha(x', 0) \partial_{x'} \gamma_\alpha(x', 0) \right\rangle_\beta, \quad (54)$$

where β is the inverse temperature and T_τ denotes time ordering. Its Fourier transform is the dynamical spin susceptibility $\chi(q, i\omega_l)$, where ω_l are bosonic Matsubara frequencies. In the calculation of the spin-lattice relaxation rate, we need the local spin susceptibility, which may be obtained as

$$\sum_q \chi_\alpha(q, i\omega_l) = \frac{L_x}{2} \int_{-\beta}^{\beta} d\tau e^{i\omega_l \tau} \tilde{\chi}_\alpha(0, \tau). \quad (55)$$

Using Wick's theorem, we can express the spin-spin correlation in terms of the Green's function $\mathcal{G}_\alpha(x, \tau) = -\langle T_\tau \gamma_\alpha(x, \tau) \gamma_\alpha(0, 0) \rangle$ for noninteracting Majorana fermions. In frequency-momentum space, we have $\mathcal{G}_\alpha(q, i\omega_n) = (i\omega_n - v_\alpha q)^{-1}$, where $v_\alpha = \alpha v$. Performing the sum over internal Matsubara frequencies, we obtain

$$\begin{aligned} \sum_q \chi_\alpha(q, i\omega_l) = \frac{s^2}{4L_x} \sum_{k_1, k_2 \geq 0} & \left\{ k_2(k_2 - k_1) \frac{f(v_\alpha k_1) - f(-v_\alpha k_2)}{i\omega_l - v_\alpha k_1 - v_\alpha k_2} + k_2(k_1 + k_2) \frac{f(v_\alpha k_1) - f(v_\alpha k_2)}{i\omega_l - v_\alpha k_1 + v_\alpha k_2} \right. \\ & \left. - k_2(k_2 + k_1) \frac{f(v_\alpha k_1) - f(v_\alpha k_2)}{i\omega_l + v_\alpha k_1 - v_\alpha k_2} - k_2(k_2 - k_1) \frac{f(v_\alpha k_1) - f(-v_\alpha k_2)}{i\omega_l + v_\alpha k_1 + v_\alpha k_2} \right\}, \end{aligned} \quad (56)$$

where $f(\omega) = (e^{\beta\omega} + 1)^{-1}$ is the Fermi-Dirac distribution. Taking the analytic continuation to real frequencies, $i\omega_l \rightarrow \omega + i0^+$ and the limit $L_x \rightarrow \infty$, we write the imaginary part of the retarded spin susceptibility as

$$-2 \sum_q \text{Im} \chi_\alpha^{\text{ret}}(q, \omega) = -\frac{s^2}{4v^2} [\mathcal{I}(\omega, T) - \mathcal{I}(-\omega, T)], \quad (57)$$

where we define the integral

$$\mathcal{I}(\omega, T) = \int_{-\infty}^{\infty} dk k(\omega + 2v_{\alpha}k) \left[f(\omega + v_{\alpha}k) - f(v_{\alpha}k) \right]. \quad (58)$$

At zero temperature, the Fermi-Dirac distribution reduces to a step function and we obtain $\mathcal{I}(\omega, 0) = -\omega^3/6v^2$. Using the Sommerfeld expansion for a quadratic function,

$$\int_{-\infty}^{\infty} d\varepsilon (A_2\varepsilon^2 + A_1\varepsilon + A_0) [f(\varepsilon - \mu) - \Theta(-\varepsilon)] = A_2 \left(\frac{\mu^3}{3} + \mu\pi^2 \frac{T^2}{3} \right) + A_1 \left(\frac{\mu^2}{2} + \pi^2 \frac{T^2}{6} \right) + A_0\mu, \quad (59)$$

we can show that

$$\mathcal{I}(\omega, T) = -\frac{\omega^3}{6v^2} - \frac{2\pi^2}{3v^2}\omega T^2. \quad (60)$$

Therefore, the dynamical spin structure factor at low temperatures is given by

$$S(q, \omega_0) \approx -\frac{2T}{\omega_0} \sum_q \text{Im}\chi_{\alpha}^{\text{ret}}(q, \omega_0) = \frac{s^2}{12v^4} \left(\omega_0^2 T + 4\pi^2 T^3 \right). \quad (61)$$